Contribution from the Paul M. Gross Chemical Laboratory,
Department of Chemistry, Duke University, Durham, North Carolina 27706

Hydroxamic Acid Ligand-Exchange Kinetics at Hexaaquoaluminum Ion

J. Mark Garrison and Alvin L. Crumbliss*

Received December 30, 1986

Hydroxamic acid (HA) ligand-exchange kinetics have been investigated at 25 °C over the $[H^+]$ range 1.0–0.001 M (I = 1.0 M ($HClO_4/NaClO_4$)). A series of five synthetic hydroxamic acids ($R_1C(O)N(OH)R_2$) were chosen for study with varying R_1 and R_2 substituents as follows: acetohydroxamic acid, $R_1 = CH_3$, $R_2 = H$; benzohydroxamic acid, $R_1 = C_6H_5$, $R_2 = H$; 4-acyl-*N*-phenylacetohydroxamic acid, $R_1 = CH_3$, $R_2 = 4\text{-}CH_3C(O)C_6H_4$; *N*-phenylacetohydroxamic acid, $R_1 = CH_3$, $R_2 = C_6H_5$; 4-methyl-*N*-phenylacetohydroxamic acid, $R_1 = CH_3$, $R_2 = 4\text{-}CH_3C_6H_4$. The kinetic results are consistent with a parallel-path reaction scheme:

$$Al(H_2O)_6^{3+} + R_1C(O)N(OH)R_2 \underset{k_{-1}}{\overset{k_1}{\rightleftharpoons}} Al(H_2O)_4(R_1C(O)N(O)R_2)^{2+} + H_3O^+ + H_2O$$

$$-H^+ \Big\downarrow \Big\uparrow H^+ \quad Q_H$$

$$Al(H_2O)_5OH^{2+} + R_1C(O)N(OH)R_2 \underset{k_{-2}}{\overset{k_2}{\rightleftharpoons}} Al(H_2O)_4(R_1C(O)N(O)R_2)^{2+} + 2H_2O$$

No proton ambiguity exists in the kinetic results due to the weak acidity of the hydroxamic acids and the relatively large hydrolysis constant (Q_H) for $Al(H_2O)_6^{3+}$. Complexation rate constants are relatively insensitive to entering group (k_1 varies from 0.15 to 0.23 M^{-1} s^{-1}; k_2 varies from 2300 to 2600 M^{-1} s^{-1}), and ligand-exchange rates at $Al(H_2O)_5OH^{2+}$ are 10^4 times faster than at $Al(H_2O)_6^{3+}$. Hydroxamic acid ligand dissociation rate constants are sensitive to leaving group (k_{-1} varies from 2.3×10^{-2} to 9.3×10^{-1} M^{-1} s^{-1}; k_{-2} varies from 4.8×10^{-3} to 1.4×10^{-1} s^{-1}), and variations in ln k_{-1} are linearly related to ln k_{-2}. These results are discussed within the context of an interchange mechanism, where complex formation energetics are dominated by water exchange at aluminum Results reported here for aluminum(III) are compared with the corresponding ligand-exchange reactions for iron(III) previously reported from our laboratory.

Introduction

The discovery that increased amounts of aluminum occur in several human brain diseases has stimulated interest in the biological role of aluminum in the body. Specifically, increased levels of aluminum have been implicated in the dialysis encephalopathy syndrome,[1] as well as neuron degeneration and Alzheimer's disease,[2] the prevalent form of senile dementia. These findings have stimulated several chelation studies of the aluminum cation with biologically important ligands using ^{27}Al NMR.[3-5] Likewise, there is now a great interest in the kinetics and equilibrium dynamics of aluminum complexation in the environment[6] due to aluminum's implication with the toxic effects of acid rain pollution on aquatic wildlife.[7-10]

The use of ^{27}Al NMR as a probe for the molecular interactions of aluminum(III) with coordinating ligands has proven to be a powerful method by which to obtain structural, thermodynamic, and kinetic information on aluminum complexes in solution.[11] Since aluminum(III) is a diamagnetic, spherically symmetric 3+ metal ion, isomorphous metal replacement of Fe(III) by Al(III) in ferrichrome[12,13] and ferrioxamine B[14] offers a proven technique by which to elucidate the solution chemistry of these metal chelating ligands and their synthetic models. Both ferrichrome and ferrioxamine B are naturally occurring siderophores synthesized by microorganisms to solubilize iron(III) from the environment and transport it to the cell.[15-17] Both contain the hydroxamic acid chelating moiety, and both solubilize iron(III) by chelation of the metal ion.

Although a significant amount of work has been done on the complexation kinetics of synthetic hydroxamic acids at high-spin iron(III),[18-24] there has been no such work reported for aluminum(III). In fact, there is a scarcity of kinetic data for ligand–H_2O substitution processes at an aquated aluminum(III) center using a series of related ligands.[25-30] It is therefore of interest to determine the kinetics and mechanism of (hydroxamato)aluminum(III) complex formation and dissociation for a series of related synthetic hydroxamic acids as shown in eq 1. The choice of specific hydroxamic acids was made so as to investigate the influence of the C- and N-substituents on the reaction kinetics. A direct comparison of these results with those obtained for the

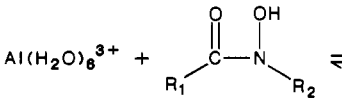

$$Al(H_2O)_4(R_1C(O)N(O)R_2)^{2+} + 2H_2O + H^+ \quad (1)$$

R_1	R_2
CH_3	H
C_6H_5	H
CH_3	$4\text{-}CH_3C(O)C_6H_4$
CH_3	C_6H_5
CH_3	$4\text{-}CH_3C_6H_4$

corresponding iron(III) system provides insight as to what property (properties) of the two metal ions influences (influence) the

* To whom correspondence should be addressed.

(1) (a) Kovalchik, M. T.; Kaehny, W. D.; Hegg, A. P.; Jackson, J. T.; Alfrey, A. C. *J. Lab. Clin. Med.* **1978**, *92*, 712. (b) Nebeker, H. G.; Coburn, J. W. *Annu. Rev. Med.* **1986**, *37*, 79. (c) Alfrey, A. C.; LeGendre, G. R.; Kaehny, W. D. *N. Engl. J. Med.* **1976**, *294*, 184.
(2) (a) Crapper, D. R.; Krishman, S. S.; Dalton, A. J. *Science (Washington, D.C.)* **1973**, *180*, 511. (b) Troncoso, J. C.; Sternberger, N. H.; Sternberger, L. A.; Hoffman, P. N.; Price, D. L. *Brain Res.* **1986**, *364*, 295. (c) Perl, D. P.; Brody, A. R. *Science (Washington, D.C.)* **1980**, *208*, 297.
(3) Tracey, A. J.; Boivin, T. L. *J. Am. Chem. Soc.* **1983**, *105*, 4901.
(4) Greenway, F. T. *Inorg. Chim. Acta* **1986**, *116*, L21.
(5) Karlik, S. J.; Elgavish, G. A.; Pillai, R. P.; Eichhorn, G. L. *J. Magn. Reson.* **1982**, *49*, 164.
(6) Plankey, B. J.; Patterson, H. H. *Environ. Sci. Technol.* **1986**, *20*, 160.
(7) Cronan, C. S.; Schofield, C. L. *Science (Washington, D.C.)* **1979**, *204*, 304.
(8) Karlsson-Norrgren, L.; Dickson, W.; Ljungberg, O.; Runn, P. *J. Fish Dis.* **1986**, *9*, 1.
(9) Anderlman, J. B.; Miller, J. R. *Water Qual. Bull.* **1986**, *11*, 19.
(10) Tam, S. C.; Williams, R. J. P. *J. Inorg. Biochem.* **1986**, *26*, 35.
(11) (a) Hinton, J. F.; Briggs, R. W. In *NMR and the Periodic Table*: Harris, R. K., Mann, B. E., Eds.; Academic: New York, 1978; pp 279–285. (b) Haraguchi, H.; Fujiwara, S. *J. Phys. Chem.* **1969**, *73*, 3467. (c) Dechter, J. J. *Prog. Inorg. Chem.* **1982**, *29*, 285. (d) Delpeuch, J. J. In *NMR of Newly Accessible Nuclei*; Laszlo, P., Ed.; Academic: New York, 1983; pp 153–195. (e) Akitt, J. W. *Annu. Rep. NMR Spectrosc.* **1972**, *5A*, 465. (f) Wehrli, F. W. *Annu. Rep. NMR Spectrosc.* **1979**, *9*, 125.
(12) Llinás, M.; Wüthrich, K. *Biochim. Biophys. Acta* **1978**, *532*, 29.
(13) Llinás, M.; DeMarco, A. *J. Am. Chem. Soc.* **1980**, *102*, 2226.
(14) Snow, G. A. *Biochem. J.* **1969**, *115*, 199.
(15) Neilands, J. B. *Microbiol. Sci.* **1984**, *1*, 9.
(16) Messenger, A. J. M.; Barclay, R. *Biochem. Educ.* **1983**, *11*, 54.
(17) Raymond, K. N.; Müller, G.; Matzanke, B. F. *Top. Curr. Chem.* **1984**, *123*, 49.
(18) Monzyk, B.; Crumbliss, A. L. *J. Am. Chem. Soc.* **1979**, *101*, 6203.
(19) Brink, C. P.; Crumbliss, A. L. *Inorg. Chem.* **1984**, *23*, 4708.

0020-1669/87/1326-3660$01.50/0

complexation kinetics of hydroxamic acids.

Experimental Section

Materials. Aqueous and 25% acetone/75% water (v/v) solutions were prepared with doubly distilled water. Aluminum nitrate (Fisher Scientific) was once-recrystallized by preparing a concentrated solution of $Al(NO_3)_3 \cdot 9H_2O$ in a 50/50 mixture of acetone/water and adding acetone (10^3-fold excess) until cloudiness persisted. Aluminum nitrate precipitated as a white microcrystalline powder upon refrigeration. Perchloric acid (70%, Mallinckrodt) was standardized by titration with 1 N NaOH (Fisher). Stock sodium perchlorate was standardized by passing an aliquot through a Dowex 50W-X8 20–50-mesh cation-exchange column and titrating the liberated H^+ to the phenolphthalein end point. Acetone (MCB) was used as received.

Hydroxamic Acids. Acetohydroxamic acid and benzohydroxamic acid were purchased from Aldrich Chemical Co. and used without further purification. *N*-Phenylacetohydroxamic acid, 4-acyl-*N*-phenylacetophydroxamic acid, and 4-methyl-*N*-phenylacetohydroxamic acid were prepared[31] and purified by flash chromatography (300-mesh silica; 85% hexane/15% ethyl acetate) of the crude product. The yellow or golden brown oil obtained was then immediately recrystallized from water. The recrystallized products were white, crystalline solids having the following melting points and TLC analyses (silica gel; 25% hexane/75% ethyl acetate): $CH_3C(O)N(OH)C_6H_5$, 66.5–67.5 °C, R_f 0.37; $CH_3C(O)N(OH)C_6H_4C(O)CH_3$, 142.5–143.5 °C, R_f 0.46; $CH_3C(O)N(OH)C_6H_4CH_3$, 73.0–73.5 °C, R_f 0.62. Elemental analyses were performed by MHW Laboratories, and the results are as follows. Anal. Found (calcd) for $CH_3C(O)N(OH)C_6H_5$: C, 64.02 (63.56); H, 6.39 (6.00); N, 9.41 (9.27). Found (calcd) for $CH_3C(O)N(OH)C_6H_4C(O)CH_3$: C, 62.33 (62.18); H, 5.99 (5.70); N, 7.29 (7.25). Found (calcd) for $CH_3C(O)N(OH)C_6H_4CH_3$: C, 65.60 (65.44); H, 8.66 (8.48); N, 6.85 (6.71).

Solution Preparation. Relaxation kinetics were studied under pseudo-first-order conditions in hydroxamic acid concentration over the $[H^+]$ range 1.0–0.001 M at 25 °C and 1.0 M ionic strength ($HClO_4/NaClO_4$). All solutions were 0.01 M in $Al(NO_3)_3 \cdot 9H_2O$ with the hydroxamic acid concentration being held constant over the $[H^+]$ range investigated. Hydroxamic acid concentrations ranged from 0.1 to 0.7 M. Acetohydroxamic acid was studied in both aqueous and 25% acetone/75% water (v/v) solutions while the other four hydroxamic acids were studied in 25% acetone/75% water (v/v) mixed-solvent solution due to solubility considerations. This mole fraction of acetone (0.075) was found to have no effect on the ligand-exchange kinetics as evidenced by comparison of rate data for $CH_3C(O)N(OH)H$ in pure H_2O and in the 25% acetone/75% H_2O (v/v) mixed-solvent system. It is also well-established that acetone does not coordinate Al^{3+}(aq) at high water/acetone mole ratios.[32-35]

^{27}Al NMR Spectra and Kinetics. ^{27}Al NMR spectra were obtained by using a JEOL Model FX-90Q spectrometer equipped with an omnitunable probe and a JEOL Model NM-TVS temperature controller. An observation frequency of 23.348 02 MHz and a pulse width of 29.0 μs (60° pulse) were employed at a spectral width of 54 Hz. The zero-filling method (SAMPO 256; Point 8192) significantly increased the signal-to-noise ratio of each spectrum and reduced data accumulation time. The use of double precision (16K memory) prevented memory overload and subsequent loss of accumulated data. All spectra were recorded after 800 scans. Line-width measurements taken on the $Al(H_2O)_6^{3+}$ resonance were determined instrumentally. Spectra taken to show slow exchange were accumulated at a spectral width of 10 kHz for an average of 20 000 scans.

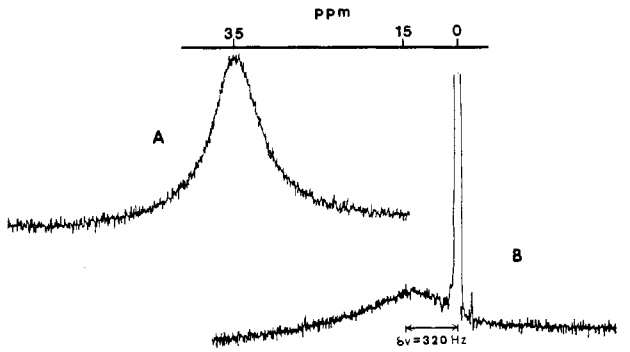

Figure 1. ^{27}Al NMR spectra at 23.348 MHz illustrating equilibrium dynamics and slow-exchange conditions for the acetohydroxamic acid/aluminum(III) system. Spectrum A shows the appearance of $Al(CH_3C(O)N(O)N)_3$ at 35 ppm under the following conditions: $[Al^{3+}] = 1.8$ M, $[CH_3C(O)N(OH)H] = 5.7$ M, $[H^+] = 10^{-5}$ M, 25 °C. Spectrum B shows the coexistence of $Al(H_2O)_4(CH_3C(O)N(O)H)^{2+}$ at 15 ppm and $Al(H_2O)_6^{3+}$ at 0 ppm in slow exchange (separation $(\delta\nu)$ 320 Hz) under the following conditions: $[Al^{3+}] = 0.9$ M, $[CH_3C(O)N(OH)H] = 4.5$ M, $[H^+] = 1.0$ M, 25 °C.

The slow-exchange condition for Al(III) kinetics was established as follows. The ^{27}Al NMR spectrum of an aqueous pH 5 solution at 25 °C containing a 3/1 molar ratio of $CH_3C(O)N(OH)H/Al^{3+}$(aq) showed a single broad resonance ($\Delta\nu_{1/2}$ = 870 Hz) 35 ppm downfield from an external $Al(D_2O)_6^{3+}$ reference standard (Figure 1), consistent with the formation of a tris(acetohydroxamato)aluminum(III) complex in solution.[13] The ^{27}Al NMR spectrum of an aqueous pH 0 solution (Figure 1) at 25 °C containing a 5/1 molar ratio of $CH_3C(O)N(OH)H/Al^{3+}$(aq), however, showed a broad, low-intensity resonance ($\Delta\nu_{1/2} \approx 1200$ Hz) at 15 ppm downfield from a sharp, higher intensity hexaaquoaluminum ion resonance. The spectral changes that occur upon increasing the acidity of a tris(acetohydroxamato)aluminum(III) solution are consistent with results found by other workers[13] and support the interpretation of the 15 ppm downfield resonance as being that of the (acetohydroxamato)aluminum(III) complex. Increasing the acidity of a tris(acetohydroxamato)aluminum(III) solution from pH 5 to pH 0 results in the protonation of hydroxamate groups and the simultaneous displacement of hydroxamic acid from the Al^{3+} coordination sphere by H_2O ligands. The fact that two separate resonances (separation 320 Hz) are observed for $Al(H_2O)_4(CH_3C(O)N(O)H)^{2+}$ and $Al(H_2O)_6^{3+}$ in acid solution indicates that the rate of H_2O/hydroxamic acid exchange between the two sites is slow relative to the ^{27}Al NMR time scale.[36]

The aquisition and analysis of kinetic data involved measuring the width at half-height of the ^{27}Al NMR resonance of $Al(H_2O)_6^{3+}$ in the absence (h_0) and in the presence (h_{ex}) of hydroxamic acid exchange at a given $[H^+]$. An observed pseudo-first-order rate constant was obtained under conditions of slow exchange[36] by use of the equation k_{obsd} (s^{-1}) = $\pi(h_{ex} - h_0)$.

Results

Hydroxamic acid relaxation kinetics have been investigated for reaction 1 at 25 °C over the $[H^+]$ range 1.0–0.001 M at an ionic strength of 1.0 M ($HClO_4/NaClO_4$). Values of k_{obsd} (s^{-1}) as a function of $[H^+]$ at various hydroxamic acid concentrations and 25 °C are compiled in Tables I–V for all five hydroxamic acid systems.[37] Figure 2 is a representative plot of these data at 25 °C for $Al(H_2O)_4(C_6H_5C(O)N(O)H)^{2+}$. The solid line in Figure 2 represents a least-squares fit of the three-parameter eq 2 to the

$$k_{obsd} = a + b/[H^+] + c[H^+] \quad (2)$$

experimental data. A good fit of eq 2 to the relaxation rate constants, k_{obsd} was obtained for all five hydroxamic acids at 25 °C.

The kinetic results are consistent with Scheme I (k_n values (n = 1, −1, 2, −2) represent microscopic rate constants, and Q_H represents the equilibrium hydrolysis constant). In contrast to

(20) Fish, L. L.; Crumbliss, A. L. *Inorg. Chem.* **1985**, *24*, 2198..
(21) Biruš, M.; Kujundžić, N.; Pribanić, M. *Inorg. Chim. Acta* **1980**, *55*, 65.
(22) Kujundžić, N.; Pribanić, M. *J. Inorg. Nucl. Chem.* **1978**, *40*, 729.
(23) Biruš, M.; Bradić, Z.; Kujundžić, N.; Pribanić, M.; Wilkins, P. C.; Wilkins, R. G. *Inorg. Chem.* **1985**, *24*, 3980.
(24) Kazmi, S. A.; McArdle, J. V. *J. Inorg. Nucl. Chem.* **1981**, *43*, 3031.
(25) Secco, F.; Venturini, M. *Inorg. Chem.* **1975**, *14*, 1978.
(26) Perlmutter-Hayman, B.; Tapuhi, E. *Inorg. Chem.* **1977**, *16*, 2742.
(27) Perlmutter-Hayman, B.; Tapuhi, E. *Inorg. Chem.* **1979**, *18*, 875.
(28) Dash, A. C. *Inorg. Chem.* **1983**, *22*, 837.
(29) Hiraishi, M.; Harada, S.; Uchida, Y.; Kuo, H. L.; Yasunaga, T. *Int. J. Chem. Kinet.* **1980**, *12*, 387.
(30) Hiraishi, M. *J. Sci. Hiroshima Univ., Ser. A: Phys. Chem.* **1980**, *44*, 311.
(31) Brink, C. P.; Crumbliss, A. L. *J. Org. Chem.* **1982**, *47*, 1171.
(32) Chi, H.; Ng, C.-H.; Li, N. C. *J. Inorg. Nucl. Chem.* **1976**, *38*, 529.
(33) Fratiello, A.; Lee, R. E.; Nishida, V. M.; Schuster, R. E. *J. Chem. Phys.* **1968**, *48*, 3705; *Inorg. Chem.* **1969**, *8*, 69.
(34) Emons, H.-H.; Pollmer, K.; Birkeneder, F. *Z. Chem.* **1984**, *24*, 73.
(35) Garrison, J. M.; Crumbliss, A. L., manuscript in preparation.
(36) (a) Becker, E. D. *High Resolution NMR*, 2nd ed.; Academic: New York, 1980; pp 240–245. (b) Abraham, R. J.; Loftus, P. *Proton and Carbon-13 NMR Spectroscopy*; Heyden: London, 1980; pp 165–168. (c) Dwek, R. A. *NMR in Biochemistry: Applications to Enzyme Systems*; Clarendon: Oxford, England, 1973; pp 37–47.
(37) See paragraph at the end of the paper regarding supplementary material.

Table VI. Microscopic Rate Constants Corresponding to Scheme I[a]

	$R_1C(O)N(OH)R_2$				
k_n	$R_1 = CH_3$, $R_2 = H$	$R_1 = C_6H_5$, $R_2 = H$	$R_1 = CH_3$, $R_2 = 4\text{-}CH_3C(O)C_6H_4$	$R_1 = CH_3$, $R_2 = C_6H_5$	$R_1 = CH_3$, $R_2 = 4\text{-}CH_3C_6H_4$
$10k_1$, $M^{-1}\ s^{-1}$	1.7 (1)	1.7 (1)	2.3 (3)	1.5 (1)	2.2 (1)
$10k_{-1}$, $M^{-1}\ s^{-1}$	3.5 (1)	9.3 (1)	1.7 (1)	1.3 (1)	0.23 (2)[b]
$10^{-3}k_2$, $M^{-1}\ s^{-1}$	2.3 (1)	2.3 (1)	2.5 (2)	2.5 (2)	2.6 (2)
10^2k_{-2}, s^{-1}	2.0 (1)	14 (1)	1.7 (4)	1.4 (2)	0.48 (9)

[a] The numbers in parentheses represent the estimated standard deviation of the least significant digit quoted. [b] A value of $4.1 \times 10^{-2}\ M^{-1}\ s^{-1}$ was obtained when kinetic data collected at $[CH_3C(O)N(OH)\text{-}4\text{-}CH_3C_6H_4] = 0.2$ and 0.3 M were used.

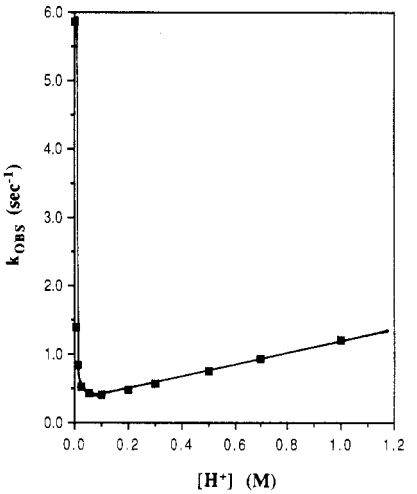

Figure 2. Plot of the observed relaxation rate constant, k_{obsd} (s^{-1}), as a function of $[H^+]$ for the $Al(H_2O)_4(C_6H_5C(O)N(O)H)^{2+}$ system where $[C_6H_5C(O)N(OH)H]_{eq} = 0.7$ M and $[Al^{3+}] = 0.01$ M ($T = 25$ °C; $I = 1.0$ M). The solid line represents a least-squares fit of eq 2 to the experimental data.

Scheme I

$$\text{path 1: } Al(H_2O)_6^{3+} + R_1C(O)N(OH)R_2 \underset{k_{-1}}{\overset{k_1}{\rightleftharpoons}}$$

$$-H^+ \Big\uparrow\Big\downarrow +H^+ \; Q_H \qquad Al(H_2O)_4(R_1C(O)N(O)R_2)^{2+} + H_2O + H_3O^+ \quad (3)$$

$$\text{path 2: } Al(H_2O)_5(OH)^{2+} + R_1C(O)N(OH)R_2 \underset{k_{-2}}{\overset{k_2}{\rightleftharpoons}}$$

$$Al(H_2O)_4(R_1C(O)N(O)R_2)^{2+} + 2H_2O \quad (4)$$

the case for several previous $Al^{3+}(aq)$ complexation studies, no proton ambiguity exists in this system. Due to the high pK_a values for the hydroxamic acid ligands,[31,38] reaction paths involving the free hydroxamate anion may be ignored over the $[H^+]$ range investigated.

When the mechanism shown in Scheme I is treated as a relaxation process at conditions where $10[Al^{3+}]_{tot} \leq [R_1C(O)N(OH)R_2]_{tot} = [R_1C(O)N(OH)R_2]_{eq}$, then eq 5 for the relaxation rate constant, k_{obsd}, may be derived. Equation 5 is of the same

$$k_{obsd} = k_1[R_1C(O)N(OH)R_2]_{eq} + k_{-2} + k_2Q_H[R_1C(O)N(OH)R_2]_{eq}/[H^+] + k_{-1}[H^+] \quad (5)$$

analytical form as eq 2, where $a = k_1[R_1C(O)N(OH)R_2]_{eq} + k_{-2}$, $b = k_2Q_H[R_1C(O)N(OH)R_2]_{eq}$, and $c = k_{-1}$. Values for the microscopic rate constants in Scheme I were obtained by rearranging eq 2 as follows:

$$[H^+]k_{obsd} = a[H^+] + b + c[H^+]^2 \quad (6)$$

A nonlinear least-squares fit of eq 6 to the kinetic data gave values for the coefficients a, b, and c for each hydroxamic acid ligand at different fixed $[R_1C(O)N(OH)R_2]_{eq}$. Values of k_1 and k_{-2} were obtained from the slope and intercept, respectively, of plots of a vs $[R_1C(O)N(OH)R_2]_{eq}$, k_2 values from b ($=k_2Q_H[R_1C(O)N(OH)R_2]_{eq}$, where $Q_H = 3.3 \times 10^{-6}$ M[39]), and k_{-1} directly from c. The microscopic rate constants corresponding to Scheme I for each hydroxamic acid investigated are listed in Table VI.

Discussion

Rate constants for (hydroxamato)aluminum(III) complex formation by either path 1 or path 2 in Scheme I are insensitive to the identity of the hydroxamic acid entering group (Table VI). Furthermore, the ratio of rate constants for all ligand substitutions at $Al(H_2O)_5OH^{2+}$ relative to those at $Al(H_2O)_6^{3+}$ ($k_2/k_1 = (1.1\text{–}1.7) \times 10^4$; Table VI) is consistent with ligand substitution at a +3 aquo and hydroxo metal ion where water-exchange energetics are dominant. For example, in the analogous iron(III) system where water-exchange rate constants have been directly measured for $Fe(H_2O)_5OH^{2+}$ and $Fe(H_2O)_6^{3+}$, the ratio $k_{ex}(Fe(H_2O)_5OH^{2+})/k_{ex}(Fe(H_2O)_6^{3+}) = 750$.[40] The rate constant ratio k_2/k_1 for hydroxamic acid ligand substitution at aqueous iron(III) falls in the appropriate range from 400 to 1700.[18,19]

The Eigen–Wilkins scheme[41] for complex formation at an aquated metal ion is

$$Al(H_2O)_6^{3+} + R_1C(O)N(OH)R_2 \underset{}{\overset{\text{fast}}{\rightleftharpoons}} \{Al(H_2O)_6,R_1C(O)N(OH)R_2\}^{3+} \quad K_{os} \quad (7)$$

$$\{Al(H_2O)_6,R_1C(O)N(OH)R_2\}^{3+} \rightleftharpoons Al(H_2O)_5(R_1C(O)N(OH)R_2)^{3+} + H_2O \quad k_i/k_{-i} \quad (8)$$

$$Al(H_2O)_5(R_1C(O)N(OH)R_2)^{3+} \rightleftharpoons Al(H_2O)_4R_1C(O)N(O)R_2^{2+} + H_3O^+ \quad k_{ii}/k_{-ii} \quad (9)$$

Step 7 represents a rapidly established equilibrium formation of an outer-sphere complex, step 8 the penetration of the hydroxamic acid into the aluminum(III) inner coordination shell, and step 9 the elimination of H_3O^+ and ring closure. Initial Al–O bond formation is assumed to occur at the carbonyl oxygen atom on the basis of the analogy with the corresponding iron(III) reactions.[18-20] Assumption of steady-state conditions for the intermediates gives the expressions

$$k_1 = \frac{K_{os}k_ik_{ii}}{k_{-i} + k_{ii}} \quad (10)$$

$$k_{-1} = \frac{k_{-ii}k_{-i}}{k_{-i} + k_{ii}} \quad (11)$$

where k_1 and k_{-1} correspond to the experimental rate constants in Table VI. Comparison of monodentate ligand complex formation rates found in the literature[6,28-30,42] with data for the bidentate hydroxamic acids suggests that ring closure is rapid (i.e. $k_{ii} \gg k_{-i}$). Consequently, eq 10 and 11 reduce to

$$k_1 = K_{os}k_i \quad (12)$$

$$k_{-1} = \frac{k_{-i}k_{-ii}}{k_{ii}} \quad (13)$$

The product $K_{os}k_i$ in eq 12 is usually diminished by a statistical correction factor ($S = {}^1/_{10}\text{–}{}^3/_4$), which takes into account the composition of the solvation shell (i.e., $k_1 = SK_{os}k_i$). K_{os} for a

(38) Monzyk, B.; Crumbliss, A. L. *J. Org. Chem.* **1980**, *45*, 4670.
(39) Baes, C. F.; Mesmer, R. E. *The Hydrolysis of Cations*; Wiley: New York, 1976; pp 112–123, 230–237.
(40) Dodgen, H. W.; Liu, G.; Hunt, J. P. *Inorg. Chem.* **1981**, *20*, 1002.
(41) Eigen, M.; Wilkins, R. G. *Adv. Chem. Ser.* **1965**, *No. 49*, 55.
(42) Miceli, J.; Stuehr, J. *J. Am. Chem. Soc.* **1968**, *90*, 6967.

Table VII. Comparison of Al(III) and Fe(III) Mono(hydroxamate) Complex Formation and Dissociation Rate Constants[a]

	$R_1C(O)N(OH)R_2$				
k_n^{Fe}/k_n^{Al}[b]	$R_1 = CH_3$, $R_2 = H$	$R_1 = C_6H_5$, $R_2 = H$	$R_1 = CH_3$, $R_2 = 4\text{-}CH_3C(O)C_6H_4$	$R_1 = CH_3$, $R_2 = C_6H_5$	$R_1 = CH_3$, $R_2 = 4\text{-}CH_3C_6H_4$
k_1^{Fe}/k_1^{Al}	7.1	26	5.2	14	10
k_2^{Fe}/k_2^{Al}	0.86	1.8	0.19	0.52	0.38
k_{-1}^{Fe}/k_{-1}^{Al}	0.29	0.037	0.071	0.052	0.33
k_{-2}^{Fe}/k_{-2}^{Al}	4.00	0.25	0.98	0.79	2.13

[a] Al(III) data from Table VI; Fe(III) data from ref 18 and 19. [b] Ratios of microscopic rate constants as defined in Scheme I.

Scheme II

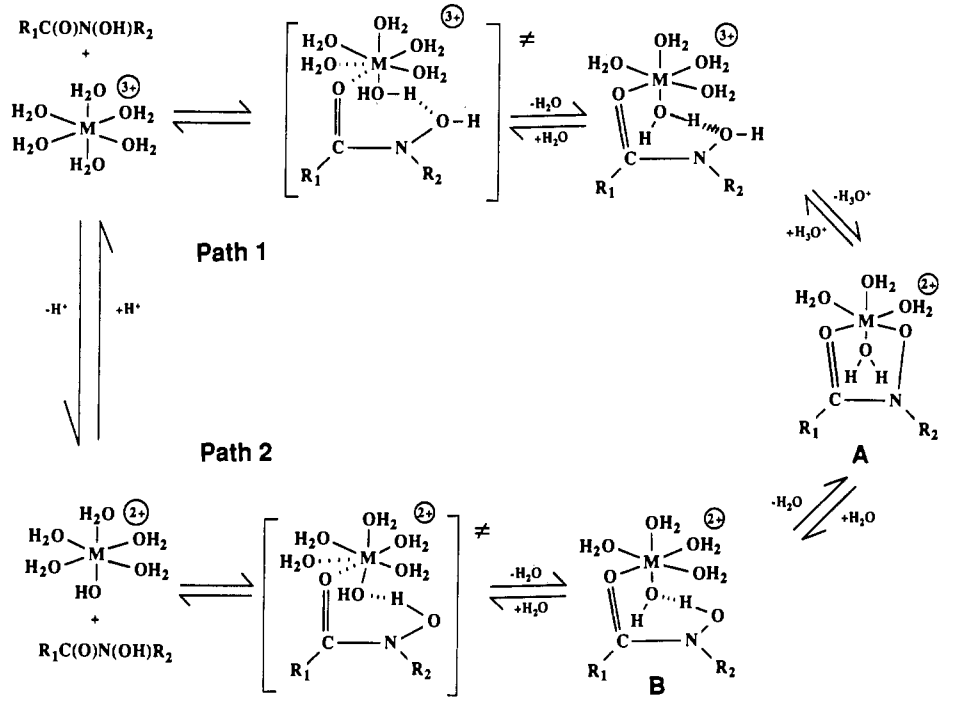

3+ cation and uncharged ligand can be estimated by use of the Fuoss equation[43] as ca. 10^{-1}.

One can therefore calculate the rate constants for ligand penetration (k_i) into the Al^{3+} inner coordination shell from the experimental values of k_1. Calculated values for k_i assuming $S = {}^3/_4$ fall in the range 2.0–3.1 s^{-1} and are in excellent agreement with the published rate of H_2O exchange for $Al(H_2O)_6^{3+}$; $k_{ex}(Al(H_2O)_6^{3+}) = 1.29\ s^{-1}$.[44] This suggests an I_d mechanism is operative for complex formation in path 1, where water-exchange energetics are dominant. Merbach et al. have assigned an I_d mechanism to water exchange at $Al(H_2O)_6^{3+}$ on the basis of a positive volume of activation for this process ($\Delta V_{ex}^{\ddagger} = +5.7\ cm^3\ mol^{-1}$).[44]

A scheme similar to that shown in eq 7–9 may be written for H_2O/hydroxamic acid ligand exchange at $Al(H_2O)_5OH^{2+}$. Direct comparison of k_2 with a water-exchange rate constant for $Al(H_2O)_5OH^{2+}$ is not possible, however, since direct measurement of this value has not been made.

A comparison of results reported here with the corresponding rate data for the same hydroxamic acid substitution reactions at $Fe(H_2O)_6^{3+}$ and $Fe(H_2O)_5OH^{2+}$ is presented in Table VII. If one makes the reasonable assumption that S and K_{os} have the same values for the Al^{3+} and Fe^{3+} reactions, then the ratios k_1^{Fe}/k_1^{Al} and k_2^{Fe}/k_2^{Al} may be directly compared with the corresponding water-exchange rate ratios for the aquo ions $M(H_2O)_6^{3+}$ and $M(H_2O)_5OH^{2+}$. The k_1^{Fe}/k_1^{Al} ratios in Table VII are low when compared with the ratio $k_{ex}(Fe(H_2O)_6^{3+})/k_{ex}(Al(H_2O)_6^{3+}) = 125$.[40,44] Although a water-exchange rate constant has not been measured for $Al(H_2O)_5OH^{2+}$, the ratios k_2^{Fe}/k_2^{Al} listed in Table VII also appear to be less than the expected ratio of $k_{ex}(Fe(H_2O)_5OH^{2+})/k_{ex}(Al(H_2O)_5OH^{2+})$. These comparisons suggest the possibility of some hydroxamic acid participation in the transition states of the Al^{3+} complexation reactions.

Both the acid-dependent (k_{-1}) and acid-independent (k_{-2}) dissociation rate constants (Table VI) show a strong dependence on leaving group. Electron-donating groups at either the R_1 or R_2 position diminish the dissociation rate constant, as was observed for the corresponding iron(III) reactions.[18,19]

Figure 3 is a plot of the logarithm of the acid-dependent aquation rate constant as a function of the logarithm of the acid-independent aquation rate constant. Also included in this plot are aquation data for the last stage of deferriferrioxamine B dissociation from aluminum(III).[45] A linear least-squares analysis of the data yields a slope of 1.0 (±0.1). For comparison purposes the corresponding data for aquation of the same hydroxamic acid ligands from iron(III)[18,19,46,47] are also plotted in Figure 3. A linear least-squares fit of these six data yields a slope of 1.1 (±0.1). Additional data for the aquation of 18 different hydroxamic acid ligands from iron(III) are available in the literature,[18–20,46,47] which extend the limits of this line while maintaining a slope of unity.

Assuming the validity of the parallel-path reaction scheme (eq 3 and 4), where the transition states differ by only a proton, it can be shown that

$$\ln k_{-1} = \ln k_{-2} + \ln\left(\frac{k_1}{k_2 Q_H}\right) \qquad (14)$$

(43) Fuoss, R. M. *J. Am. Chem. Soc.* **1958**, *80*, 5059. Prue, J. E. *J. Chem. Educ.* **1969**, *46*, 12.
(44) Hugi-Cleary, D.; Helm, L.; Merbach, A. E. *Helv. Chim. Acta* **1985**, *68*, 545.
(45) Garrison, J. M.; Crumbliss, A. L. *Inorg. Chim. Acta* **1987**, *138*, 61.
(46) Monzyk, B.; Crumbliss, A. L. *Inorg. Chim. Acta* **1981**, *55*, L5.
(47) Monzyk, B.; Crumbliss, A. L. *J. Am. Chem. Soc.* **1982**, *104*, 4921.

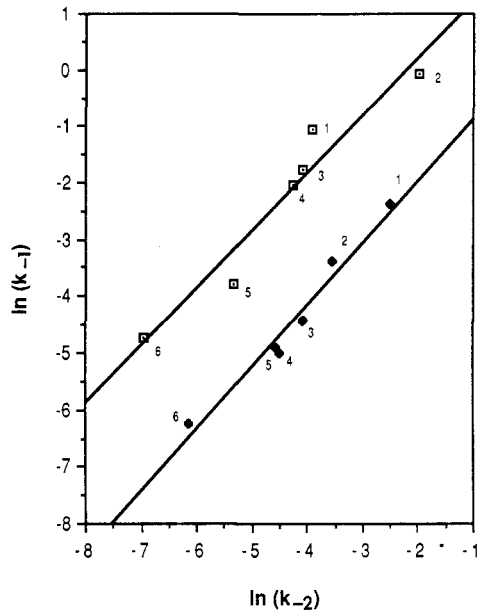

Figure 3. Plot of the natural logarithm of the acid-dependent aquation rate constant, ln k_{-1}, as a function of the acid-independent rate constant, ln k_{-2}, for a series of six hydroxamic acid/aluminum(III) systems. The corresponding data for aquation of the same hydroxamic acid ligands from iron(III) are included for comparison purposes.[18,19,46,47] Numbered data correspond to hydroxamic acids ($R_1C(O)N(OH)R_2$) as follows: (1) $R_1 = CH_3$, $R_2 = H$; (2) $R_1 = C_6H_5$, $R_1 = H$; (3) $R_1 = CH_3$, $R_2 = 4\text{-}CH_3C(O)C_6H_4$; (4) $R_1 = CH_3$, $R_2 = C_6H_5$; (5) $R_1 = CH_3$, $R_2 = 4\text{-}CH_3C_6H_4$; (6) deferriferrioxamine B (H_3DFB), $CH_3[C(O)N(OH)(CH_2)_5C(O)NH(CH_2)_2]_2C(O)N(OH)(CH_2)_5NH_2$.[45-47] Open squares represent $Al(H_2O)_4(R_1C(O)N(O)R_2)^{2+}$ and $Al(H_3DFB)^{3+}$ data: slope 1.01 (±0.13), intercept 2.24 (±0.61), correlation coefficient 0.94. Solid diamonds represent $Fe(H_2O)_4(R_1C(O)N(O)R_2)^{2+}$ and $Fe(H_3DFB)^{3+}$ data: slope 1.09 (±0.10), intercept 0.234 (±0.431), correlation coefficient 0.97.

Consequently, if for a series of hydroxamic acid ligands the ratio k_1/k_2Q_H is relatively constant, then ln k_{-1} and ln k_{-2} should be linearly correlated with a slope of 1, as shown in Figure 3. The larger intercept observed for the series of aquation reactions for Al(III) is consistent with a smaller hydrolysis constant (Q_H) for $Al(H_2O)_6^{3+}$ relative to that for $Fe(H_2O)_6^{3+}$ and the relative k_1/k_2 values observed for the Al(III) and Fe(III) reactions. The linear correlations shown in Figure 3 confirm the validity of Scheme I and the direct mechanistic correlation between hydroxamic acid reactions with $Al(H_2O)_6^{3+}$ and $Fe(H_2O)_6^{3+}$.

The mechanism for hydroxamate complex formation and dissociation for iron(III) and aluminum(III) is illustrated in Scheme II. Complex formation occurs as an interchange process with initial bond formation occurring at the carbonyl oxygen atom. Complex formation is slower for Al^{3+} than for Fe^{3+} in both path 1 and path 2 due to slower rates of water exchange for Al^{3+}.[40,44] As shown previously for $Fe(H_2O)_4(R_1C(O)N(O)R_2)^{2+}$ aquation reactions,[18-20] we propose that initial bond cleavage for the aquation reaction occurs at

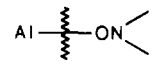

as shown. In the acid-independent aquation path (path 2), an internal hydrolysis occurs on proceeding from the hydroxamate complex (A in Scheme II) to the half-chelated intermediate (B in Scheme II). This is consistent with the known acidities of aquated Al(III) and Fe(III)[39] and the hydroxamic acids.[31,38] An intermediate or transition-state structure that illustrates this internal hydrolysis that would occur in the process A → B in Scheme II is shown by I. That this intramolecular proton transfer is less

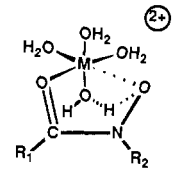

I

efficient for the aluminum(III) reactions can be seen from Figure 3, where the intercept is greater for the aluminum(III) correlation (partially due to the relative Q_H values for $Al(H_2O)_6^{3+}$ and $Fe(H_2O)_6^{3+}$). This same effect is seen in Table VII, where for each hydroxamic acid studied the inequality shown in (15) holds true.

$$\frac{k_{-2}^{Fe}}{k_{-2}^{Al}} > \frac{k_{-1}^{Fe}}{k_{-1}^{Al}} \qquad (15)$$

That is, for all hydroxamic acids, dissociation via path 2 is relatively less efficient in the Al^{3+} system. This is due to the less efficient intramolecular proton transfer for Al^{3+} shown by I above, due to its lesser tendency to undergo hydrolysis.[39]

Acknowledgment is made to the donors of the Petroleum Research Fund, administered by the American Chemical Society, for support of this research.

Registry No. $R_1C(O)N(OH)R_2$ ($R_1 = CH_3$, $R_2 = H$), 546-88-3; $R_1C(O)N(OH)R_2$ ($R_1 = C_6H_5$, $R_2 = H$), 495-18-1; $R_1C(O)N(OH)R_2$ ($R_1 = CH_3$, $R_2 = 4\text{-}CH_3C(O)C_6H_4$), 67274-51-5; $R_1C(O)N(OH)R_2$ ($R_1 = CH_3$, $R_2 = C_6H_5$), 1795-83-1; $R_1C(O)N(OH)R_2$ ($R_1 = CH_3$, $R_2 = 4\text{-}CH_3C_6H_4$), 27451-21-4; $Al(H_2O)_6$, 15453-67-5.

Supplementary Material Available: Tables I–V, giving rate constant data (5 pages). Ordering information is given on any current masthead page.